

Appendix A Geometry for Aerodynamicists

Aerodynamicists control the flowfield through geometry definition, and are always interested in possible geometric shapes that would be useful in design. This appendix provides the detailed definition of many of the classic shapes frequently specified in aerodynamics. It is not encyclopedic. Section A.1.1 gives some other sources for airfoils.

A.1 Airfoil Geometry

The NACA Airfoils

The NACA airfoils were designed during the period from 1929 through 1947 under the direction of Eastman Jacobs at the NACA's Langley Field Laboratory. Most of the airfoils were based on simple geometrical descriptions of the section shape, although the 6 and 6A series were developed using theoretical analysis and don't have simple shape definitions. Although a new generation of airfoils has emerged as a result of improved understanding of airfoil performance and the ability to design new airfoils using computational methods, the NACA airfoils are still useful in many aerodynamic design applications. A number of references have been included to allow the reader to study both the older NACA literature and the new airfoil design ideas. Taken together, this literature provides a means of obtaining a rather complete understanding of the ways in which airfoils can be shaped to obtain desired performance characteristics.

The NACA airfoils are constructed by combining a thickness envelope with a camber or mean line. The equations that describe this procedure are:

$$\begin{aligned}x_u &= x - y_t(x) \sin \theta \\y_u &= y_c(x) + y_t(x) \cos \theta\end{aligned}\tag{A-1}$$

and

$$\begin{aligned}x_l &= x + y_t(x) \sin \theta \\y_l &= y_c(x) - y_t(x) \cos \theta\end{aligned}\tag{A-2}$$

where $y_t(x)$ is the thickness function, $y_c(x)$ is the camber line function, and

$$\theta = \tan^{-1} \left(\frac{dy_c}{dx} \right)\tag{A-3}$$

is the camber line slope. It is not unusual to neglect the camber line slope terms in Eqns. A-1 and A-3. This simplifies the equations and makes the reverse problem of extracting the thickness envelope and mean line for a given airfoil straightforward.

The primary reference volume for all the NACA subsonic airfoil studies remains:

Abbott, I.H., and von Doenhoff, A.E., *Theory of Wing Sections*, Dover, 1959.

The following paragraphs provide a brief history of the development of the NACA Airfoils. References to the development of the NASA advanced airfoils, which were developed from 1966 to approximately 1977 are given below also. The original NACA Reports are now available as pdf files through NASA, and are well worth reading.

<u>Evolution of the NACA airfoils</u>	<u>Primary NACA Report</u>	<u>Authors</u>	<u>Date</u>
1. <i>The 4-digit foils</i> : According to Abbott, Pinkerton found that the thickness distribution of the Clark Y and Gottingen 398 airfoils were similar, and Jacobs selected a function to describe this thickness distribution. The mean lines were selected to be described by two parabolic arcs which were tangent at the position of maximum camber.	R-460	Jacobs, Ward and Pinkerton	1933
2. <i>The 4-digit modified foils</i> : The camber lines were identical to the 4-digit series, and a more general thickness distribution was defined, which allowed variations in the leading edge radius and position of maximum thickness to be investigated.	R-492	Stack and von Doenhoff	1934
3. <i>The 5-digit foils</i> : The thickness distribution was kept identical to the 4-digit series, and a new camber line was defined which allowed for camber to be concentrated near the leading edge. A reflexed camber line was designed to produce zero pitching moment, but has generally not been used. These foils were derived to get good high lift with minimum C_{m0} .	R-537 R-610	Jacobs, Pinkerton and Greenberg	1935 1937
4. <i>The 6-series foils</i> : The foils were designed to maintain laminar flow over a large portion of the chord by delaying the adverse pressure gradient. The thickness envelope was obtained using exact airfoil theory, and no simple formulas are available to describe the shapes. The camber lines were designed using thin airfoil theory and simple formulas are available which describe their shape.	R-824*	Abbott, von Doenhoff and Stivers	1945
5. <i>The 6A-series foils</i> : To improve the trailing edge structurally, the 6-series foils were redesigned to provide sections with simple (nearly straight) surface geometry near the trailing edge, while maintaining the same general properties as the original foils. The camber line can be described by a simple alteration of the standard 6-series mean line.	R-903*	Loftin	1948

These airfoils, in virtually any combination of camber lines and thickness envelopes, can be constructed using program FOILGEN, described in App. E.

Historical accounts of the NACA airfoil program are contained in:

Abbott, I.H., "Airfoils," *Evolution of Aircraft Wing Design*, AIAA Dayton Section Symposium, March 1980, AIAA Paper 80-3033.

* Additional section data is contained in NASA R-84, 1958, by Patterson and Braslow.

The maximum thickness occurs at $x/c = 0.30$, and the leading edge radius is

$$\left(\frac{r_{LE}}{c}\right) = 1.1019\left(\frac{t}{c}\right)^2 \quad (A-5)$$

The included angle of the trailing edge is:

$$\delta_{TE} = 2 \tan^{-1} \left\{ 1.16925 \left(\frac{t}{c}\right) \right\} \quad (A-6)$$

As noted above, it is important to realize that the airfoil has a finite thickness at the trailing edge.

The camber line is given by:

$$\left. \begin{aligned} \frac{y_c}{c} &= \frac{M}{P^2} \left[2P(x/c) - (x/c)^2 \right] \\ \frac{dy_c}{dx} &= \frac{2M}{P^2} (P - (x/c)) \end{aligned} \right\} \left(\frac{x}{c}\right) < P \quad (A-7)$$

and

$$\left. \begin{aligned} \frac{y_c}{c} &= \frac{M}{(1-P)^2} \left[1 - 2P + 2P(x/c) - (x/c)^2 \right] \\ \frac{dy_c}{dx} &= \frac{2M}{(1-P)^2} (P - (x/c)) \end{aligned} \right\} \left(\frac{x}{c}\right) \geq P \quad (A-8)$$

The camber line slope is found from Eqn. A-3 using Eqns. A-7 and A-8, and the upper and lower surface ordinates resulting from the combination of thickness and camber are then computed using equations Eqns. A-1 and A-2.

The NACA 5-Digit Airfoil

This airfoil is an extension of the 4 digit series that provides additional camber lines. The numbering system for these airfoils is defined by:

NACA LPQXX

where XX is the maximum thickness, t/c , in percent chord.

- L is the amount of camber; the design lift coefficient is $3/2 L$, in tenths
- P is the designator for the position of maximum camber, x_f , where $x_f = P/2$, and P is given in tenths of the chord
- Q = 0; standard 5 digit foil camber
= 1; "reflexed" camber

An example: the NACA 23012, is a 12% thick airfoil, the design lift coefficient is 0.3, the position of max camber is located at $x/c = 0.15$, and the “standard” 5 digit foil camber line is used.

The thickness distribution is the same as the NACA 4 digit airfoil thickness distribution described above in equation (A-4).

The standard five-digit series camber line is given by:

$$\left. \begin{aligned} \frac{y_c}{c} &= \frac{K_1}{6} \left[(x/c)^3 - 3m(x/c)^2 + m^2(3-m)(x/c) \right] \\ \frac{dy_c}{dx} &= \frac{K_1}{6} \left[3(x/c)^2 - 6m(x/c) + m^2(3-m) \right] \end{aligned} \right\} 0 \leq (x/c) \leq m \quad (\text{A-9})$$

and

$$\left. \begin{aligned} \frac{y_c}{c} &= \frac{K_1}{6} m^3 \left[1 - (x/c) \right] \\ \frac{dy_c}{dx} &= -\frac{K_1}{6} m^3 \end{aligned} \right\} m < (x/c) \leq 1 \quad (\text{A-10})$$

where m is not the position of maximum camber, but is related to the maximum camber position by:

$$x_f = m \left(1 - \sqrt{\frac{m}{3}} \right) \quad (\text{A-11})$$

and m is found from a simple fixed point iteration for a given x_f . K_1 is defined to avoid the leading edge singularity for a prescribed C_{li} and m :

$$K_1 = \frac{6C_{li}}{Q} \quad (\text{A-12})$$

where:

$$Q = \frac{3m - 7m^2 + 8m^3 - 4m^4}{\sqrt{m(1-m)}} - \frac{3}{2}(1-2m) \left[\frac{\pi}{2} - \sin^{-1}(1-2m) \right] \quad (\text{A-13})$$

Note that K_1 is a linear function of C_{li} and the K_1 's were originally tabulated for $C_{li} = 0.3$. The tabulated K_1 's are multiplied by $(C_{li}/0.3)$ to get values at other C_{li} . To compute the camber line, the values of Q and K_1 must be determined. In some cases the computed values of K_1 and Q differ slightly from the official tabulated values (remember these were computed in the 1930s). The tabulated values should be used to reproduce the official ordinates. The following table illustrates the differences.

Mean Line	x_f	m		K_1		
		tabulated	computed	tabulated	using tabulated m	using computed m
210	0.05	0.0580	0.0581	361.4	351.56	350.332
220	0.10	0.1260	0.1257	51.65	51.318	51.578
230	0.15	0.2025	0.2027	15.65	15.955	15.920
240	0.20	0.2900	0.2903	6.643	6.641	6.624
250	0.25	0.3910	0.3913	3.230	3.230	3.223

Once the camberline parameters are chosen, the airfoil is constructed using the equations given above.

Camber lines designed to produce zero pitching moment.

The reflexed mean line equations were derived to produce zero pitching moment about the quarter chord.

$$\frac{y_c}{c} = \frac{K_1}{6} \left[\{(x/c) - m\}^3 - \frac{K_2}{K_1} (1-m)^3 (x/c) - m^3 (x/c) + m^3 \right] \quad 0 \leq (x/c) \leq m \quad (A-14)$$

$$= \frac{K_1}{6} \left[\frac{K_2}{K_1} \{(x/c) - m\}^3 - \frac{K_2}{K_1} (1-m)^3 (x/c) - m^3 (x/c) + m^3 \right] \quad m < (x/c) \leq 1 \quad (A-15)$$

where

$$\frac{K_2}{K_1} = \frac{3(m - x_f)^2 - m^3}{(1-m)^3} \quad (A-16)$$

The parameters are defined as follows: i) given x_f , find m to give $C_{mc/4} = 0$ from thin airfoil theory; ii) given x_f and m , calculate K_1 to give $C_{li} = 0.3$.

The tabulated values for these camber lines are:

Mean Line	(P/2) x_f	m	K_1	K_1/K_2
211	.05	-	-	-
221	.10	0.1300	51.99	0.000764
231	.15	0.2170	15.793	0.006770
241	.20	0.3180	6.520	0.030300
251	.25	0.4410	3.191	0.135500

The NACA Modified 4-Digit Airfoil

This airfoil is an extension of the 4-digit series to allow for a variation of leading edge radius and location of maximum thickness. The numbering system is defined by:

NACA MPXX-IT

where MPXX is the standard 4-digit designation and the IT appended at the end describes the modification to the thickness distribution. They are defined as:

I - designation of the leading edge radius

T - chordwise position of maximum thickness in tenths of chord

$$\frac{r_{le}}{c} = 1.1019 \left(\frac{I}{6} \cdot \frac{t}{c} \right)^2 \quad \text{for } I \leq 8 \quad (\text{A-17})$$

and

$$\frac{r_{le}}{c} = 3 \times 1.1019 \left(\frac{t}{c} \right)^2 \quad \text{for } I = 9 \quad (\text{A-18})$$

$I = 6$ produces the leading edge radius of the standard 4-digit airfoils.

An example: NACA 0012-74 denotes an uncambered 12% thick airfoil, with a maximum thickness at $x/c = 0.40$ and a leading edge radius of 0.0216, which is 36% larger than the standard 4-digit value.

The NACA 16 series is a special case of the modified 4-digit airfoil with a leading edge radius index of $I = 4$ and the maximum thickness located at $x/c = 0.5$ ($T = 5$). As an example, the NACA 16-012 is equivalent to an NACA 0012-45.

The thickness distribution is given by:

$$\frac{y_t}{c} = 5 \left(\frac{t}{c} \right) \left[a_0 \sqrt{\frac{x}{c}} + a_1 \left(\frac{x}{c} \right) + a_2 \left(\frac{x}{c} \right)^2 + a_3 \left(\frac{x}{c} \right)^3 \right] \quad 0 < \frac{x}{c} < T \quad (\text{A-19})$$

and

$$\frac{y_t}{c} = 5 \left(\frac{t}{c} \right) \left[.002 + d_1 \left(1 - \frac{x}{c} \right) + d_2 \left(1 - \frac{x}{c} \right)^2 + d_3 \left(1 - \frac{x}{c} \right)^3 \right] \quad T < \frac{x}{c} \leq 1 \quad (\text{A-20})$$

The coefficients are determined by solving for the d 's first, based on the trailing edge slope and the condition of maximum thickness at $x/c = T$. Once these coefficients are found, the a 's are found by relating a_0 to the specified leading edge radius, the maximum thickness at $x/c = T$, and the condition of continuity of curvature at $x/c = T$. These constants are all determined for $t/c = 0.2$, and then scaled to other t/c values by multiplying by $5(t/c)$. The value of d_1 controls the trailing edge slope and was originally selected to avoid reversals of curvature. In addition to the tabulated values, Riegels has provided an interpolation formula. The official (tabulated) and Riegels approximate values of d_1 are given in the following table.

T	Tabulated d_1	Approximate d_1
0.2	0.200	0.200
0.3	0.234	0.234
0.4	0.315	0.314
0.5	0.465	0.464
0.6	0.700	0.722

where the Riegels approximation is given by:

$$d_1 \cong \frac{(2.24 - 5.42T + 12.3T^2)}{10(1 - 0.878T)} \quad (\text{A-21})$$

Once the value of d_1 is known, d_2 and d_3 are found from the relations given by Riegels:

$$d_2 = \frac{0.294 - 2(1 - T)d_1}{(1 - T)^2} \quad (\text{A-22})$$

and

$$d_3 = \frac{-0.196 + (1 - T)d_1}{(1 - T)^3} \quad (\text{A-23})$$

With the d 's determined, the a 's can be found. a_0 is based on the leading edge radius:

$$a_0 = 0.296904 \cdot \chi_{LE} \quad (\text{A-24})$$

where

$$\begin{aligned} \chi_{LE} &= \frac{I}{6} && \text{for } I \leq 8 \\ &= 10.3933 && \text{for } I = 9 \end{aligned} \quad (\text{A-25})$$

Defining:

$$\rho_1 = \left(\frac{1}{5}\right) \frac{(1 - T)^2}{[0.588 - 2d_1(1 - T)]} \quad (\text{A-26})$$

the rest of the a 's can be found from:

$$a_1 = \frac{0.3}{T} - \frac{15}{8} \cdot \frac{a_0}{\sqrt{T}} - \frac{T}{10\rho_1} \quad (\text{A-27})$$

$$a_2 = -\frac{0.3}{T^2} + \frac{5}{4} \cdot \frac{a_0}{T^{3/2}} + \frac{1}{5\rho_1} \quad (\text{A-28})$$

$$a_3 = \frac{0.1}{T^3} - \frac{0.375a_0}{T^{5/2}} - \frac{1}{10\rho_1 T} \quad (\text{A-29})$$

The camber lines are identical to the standard 4-digit airfoils described previously. The upper and lower ordinates are then computed using the standard equations.

The NACA 6 and 6A-Series Mean Lines*

The 6-series mean lines were designed using thin airfoil theory to produce a constant loading from the leading edge back to $x/c = a$, after which the loading decreases linearly to zero at the trailing edge. Theoretically, the loading at the leading edge must be either zero or infinite within the context of thin airfoil theory analysis. The violation of the theory by the assumed finite leading edge loading is reflected by the presence of a weak singularity in the mean line at the leading edge, where the camber line has an infinite slope. Therefore, according to Abbott and von Doenhoff, the 6-series airfoils were constructed by holding the slope of the mean line constant in front of $x/c = 0.005$, with the value at that point. For round leading edges the camberline values are essentially not used at points ahead of the origin of the leading edge radius. The theory is discussed by Abbott and von Doenhoff on pages 73-75, 113, and 120. Tabulated values are contained on pages 394-405. The derivation of this mean line is a good exercise in thin airfoil theory.

By simply adding various mean lines together, other load distributions can be constructed.

From Abbott and von Doenhoff: “The NACA 6-series wing sections are usually designated by a six-digit number together with a statement showing the type of mean line used. For example, in the designation NACA 65,3-218, $a = 0.5$, the 6 is the series designation. The 5 denotes the chordwise position of minimum pressure in tenths of the chord behind the leading edge for the basic symmetrical section at zero lift. The 3 following the comma (sometimes this is a subscript or in parenthesis) gives the range of lift coefficient in tenths above and below the design lift coefficient in which favorable pressure gradients exist on both surfaces. The 2 following the dash gives the design lift coefficient in tenths. The last two digits indicate the thickness of the wing section in percent chord. The designation $a = 0.5$ shows the type of mean line used. When the mean-line is not given, it is understood that the uniform-load mean line ($a = 1.0$) has been used.”

The 6A series airfoils employed an empirical modification of the $a = 0.8$ camberline to allow the airfoil to be constructed of nearly straight line segments near the trailing edge. This camberline is described by Loftin in NACA R-903.

Basic Camberline Equations

When $a = 1$ (uniform loading along the entire chord):

$$\frac{y}{c} = -\frac{C_{l_i}}{4\pi} \left[\left(1 - \frac{x}{c}\right) \ln \left(1 - \frac{x}{c}\right) + \frac{x}{c} \ln \left(\frac{x}{c}\right) \right] \quad (\text{A-30})$$

and

$$\frac{dy}{dx} = \frac{C_{l_i}}{4\pi} \left[\ln \left(1 - \frac{x}{c}\right) - \ln \left(\frac{x}{c}\right) \right] \quad (\text{A-31})$$

* Only the mean lines have analytical definitions. The thickness distributions are the result of numerical methods which produced tabulated coordinates. In addition to the values tabulated in the NACA reports, the closest approximation for the thickness distributions is available in program LADSON, see App. E.

where C_{li} is the “ideal” or design lift coefficient, which occurs at zero angle-of-attack. For $a < 1$,

$$\frac{y}{c} = \frac{C_{li}}{2\pi(1+a)} \left\{ \begin{array}{l} \frac{1}{1-a} \left[\frac{1}{2} \left(a - \frac{x}{c} \right)^2 \ln \left| a - \frac{x}{c} \right| - \frac{1}{2} \left(1 - \frac{x}{c} \right)^2 \ln \left(1 - \frac{x}{c} \right) \right] \\ + \frac{1}{4} \left(1 - \frac{x}{c} \right)^2 - \frac{1}{4} \left(a - \frac{x}{c} \right)^2 \\ - \frac{x}{c} \ln \left(\frac{x}{c} \right) + g - h \frac{x}{c} \end{array} \right\} \quad (\text{A-32})$$

with

$$g = \frac{-1}{(1-a)} \left[a^2 \left(\frac{1}{2} \ln a - \frac{1}{4} \right) + \frac{1}{4} \right] \quad (\text{A-33})$$

$$h = (1-a) \left[\frac{1}{2} \ln(1-a) - \frac{1}{4} \right] + g \quad (\text{A-34})$$

and

$$\frac{dy}{dx} = \frac{C_{li}}{2\pi(1+a)} \left\{ \frac{1}{1-a} \left[\left(1 - \frac{x}{c} \right) \ln \left(1 - \frac{x}{c} \right) - \left(a - \frac{x}{c} \right) \ln \left(a - \frac{x}{c} \right) \right] - \ln \left(\frac{x}{c} \right) - 1 - h \right\} \quad (\text{A-35})$$

The associated angle-of-attack is:

$$\alpha_i = \frac{C_{li} h}{2\pi(1+a)} \quad (\text{A-36})$$

$a = .8$ (modified), the 6A-series mean line

For $0 < x/c < .87437$, use the basic $a = .8$ camberline, but with a modified value of the ideal lift coefficient, $C_{li\text{mod}} = C_{li}/1.0209$. For $.87437 < x/c < 1$, use the linear equation:

$$\frac{y_c/c}{C_{li}} = 0.0302164 - 0.245209 \left(\frac{x}{c} - 0.87437 \right) \quad (\text{A-37})$$

and

$$\frac{dy}{dx} = -0.245209 C_{li} \quad (\text{A-38})$$

Note that at $x/c = 1$, the foregoing approximate relation gives $y/c = -0.000589$, indicating an α shift of $.034^\circ$ for $C_{li} = 1$.

Other airfoil definition procedures

Interest in defining airfoils by a small number of parameters for use in numerical optimization has led to several recent proposed parametric representations that might be useful. In particular, the work by August and co-workers at McDonnell Douglas in St. Louis, MO, uses Chebyshev functions to obtain functions which can represent very general airfoil shapes with from 5 to 20 coefficients required. This work is described in AIAA Papers 93-0099 and 93-0100, "An Efficient Approach to Optimal Aerodynamic Design," Parts 1 and 2.

Another approach using Bezier methods frequently used in CAD surface representation software has been used by Ventkataraman. This approach uses 14 design variables to represent the airfoil, and is described in AIAA Paper 95-1875, "A New Procedure for Airfoil Definition," and AIAA Paper 95-1876, "Optimum Airfoil Design in Viscous Flows." Smith and co-workers at NASA Langley have used a similar approach based on non-uniform rational B-splines (NURBS). A description of their approach appears in AIAA Paper 93-0195, "Grid and Design Variables Sensitivity Analysis for NACA Four-Digit Wing-Sections."

A.1.1. Tabulated Airfoil Definition and the Airfoil Library

Most modern airfoils are not described by equations, but are defined by a table of coordinates. Frequently, these coordinates are the results of a computational aerodynamic design program, and simple algebraic formulas cannot be used to define the shape (this was the case with the NACA 6-series airfoils described above). The following table provides a list of the tabulated airfoils currently available on the web site. The subsequent tables provide a guide to these airfoils. A standard 2F10 format (the Jameson input format) is used with each set of coordinates. The values are given from leading edge to trailing edge, top followed by bottom.

Airfoil Library Files:

	<u>file name</u>	<u>comments</u>
NACA 4 digit airfoils		
NACA 0010	N0010.DAT	
NACA 0010-35	N001035.DAT	(Abbott & VonDoenhoff)
NACA 0012	N0012.DAT	
NACA 4412	N44122.DAT	
NACA 6 & 6A airfoils		
NACA 63(2)-215	N632215.DAT	NASA TM 78503
NACA 63(2)-215 mod B	N632215m.DAT	
NACA 64A010	N64A010.DAT	
NACA 64A410*	N64A410.DAT	
NACA 64(3)-418	N643418.DAT	
NACA 65(1)-012	N651012.DAT	
NACA 65(1)-213	N651213.DAT	
NACA 65(1)A012	N65A012.DAT	
	N658299M.DAT	
	N658299R.DAT	
NACA 65(2)-215	N652215.DAT	
NACA 66(3)-018	N663018.DAT	
NASA General Aviation Series		
LS(1)-0417	GAW1.DAT	originally known as: GA(W)-1
LS(1)-0417 mod	LS10417M.DAT	
LS(1)-0413	GAW2.DAT	originally known as: GA(W)-2
LS(1)-0013	LS10013.DAT	
NASA Medium Speed Series		
MS(1)-0313	MS10313.DAT	
MS(1)-0317	MS10317.DAT	

* Be aware that the coordinates for this airfoil, widely used as a test case, on page 356 of the book by Abbott and von Doenhoff, contain some typos. In particular, the value of y at $x = 7.5$ is supposed to be 2.805. Also, it is obvious that the x value between 30 and 40 is 35. Finally, the table is mislabeled. The y typo was responsible for the widely circulated story that the coordinates contained in Abbott and von Doenhoff were not accurate enough to be use in modern computational airfoil codes.

Airfoil Library Files (continued):

	<u>file name</u>	<u>comments</u>
NASA Laminar Flow Series		
NLF(1)-1215F	NL11215F.DAT	
NLF(1)-0414F	NL10414F.DAT	
NLF(1)-0416	NL10416.DAT	
NLF(1)-0414Fmod	NL0414FD.DAT	drooped le
NLF(2)-0415	NL20415.DAT	
HSNLF(1)-0213	HSN0213.DAT	
HSNLF(1)-0213mod	HSN0213D.DAT	drooped le
NASA Supercritical Airfoils*		
SC(2)-0402	SC20402.DAT	
SC(2)-0403	SC20403.DAT	
SC(2)-0503	SC20503.DAT	
SC(2)-0404	SC20404.DAT	
SC(2)-0406	SC20406.DAT	
SC(2)-0606	SC20606.DAT	
SC(2)-0706	SC20706.DAT	
SC(2)-1006	SC21006.DAT	
SC(2)-0010	SC20010.DAT	
SC(2)-0410	SC20410.DAT	
SC(2)-0610	SC20610.DAT	
SC(2)-0710	SC20710.DAT	also known as Foil 33
SC(2)-1010	SC21010.DAT	
SC(2)-0012	SC20012.DAT	
SC(2)-0412	SC20412.DAT	
SC(2)-0612	SC20612.DAT	
SC(2)-0712	SC20712.DAT	
SC(3)-0712(B)	SC20712B.DAT	
SC(2)-0414	SC20414.DAT	
SC(2)-0614	SC20614.DAT	
SC(2)-0714	SC20714.DAT	Raymer, Ref. NASA TP 2890
SC(2)-0518	SC20518.DAT	
FOIL31	FOIL31.DAT	
SUPER11	SUPER11.dat	11% thick, from ICAS paper
SUPER14	SUPER14.dat	14% thick, NASA TM X-72712
NYU Airfoils		
82-06-09	K820609.DAT	
79-03-12	K790312.DAT	
72-06-16	K720616.DAT	
71-08-14	K710814.DAT	
70-10-13	K701013.DAT	
65-14-08	K651408.DAT	
65-15-10	K651510.DAT	
75-06-12	KORN.DAT	the "Korn" Airfoil
75-07-15	K750715.DAT	

* These coordinates were typed in by students when NASA TP 2969 was issued. They are exactly the values printed in the TP. It turns out that those values were developed by taking the original set of coordinates and enhancing them to 100 points upper and lower using straight line interpolation. As such, they are not really usable. Our experience is that we can identify the original values and weed out the straight-line interpolated values. This works.

Airfoil Library Files (continued):

	<u>file name</u>	<u>comments</u>
<i>Miscellaneous Transonic Airfoils</i>		
CAST 7	CAST7.DAT	
DSMA 523	DSMA523.DAT	from AIAA Papre 75-880
NLR HT 731081	NLRHT73.DAT	from AGARD AR-138
ONERA M6	ONERAM6.DAT	
RAE 2822	RAE2822.DAT	
WILBY A	WILBYA.DAT	
WILBY B	WILBYB.DAT	
WILBY C	WILBYC.DAT	
WILBY R	WILBYR.DAT	
SUPER10	NASA10SC.DAT	AGARD AR-138
	MBB-A3.DAT	AGARD AR-138
<i>Eppler Airfoils</i>		
EPPLER 662	EPP662.DAT	Raymer's book, ref NASA CP 2085
EPPLER 746	EPP746.DAT	Raymer's book, ref NASA CP 2085
<i>Wortman Airfoils</i>		
FX-63-137-ESM	FX63137.DAT	
FX-72-MS-150A	FX72M15A.DAT	
FX-72-MS-150B	FX72M15B.DAT	
<i>Miscellaneous Foils</i>		
ClarkY	CLARKY.DAT	
Early Liebeck High Lift	RHLHILFT.DAT	
NLR-1	NLR1.DAT	Rotorcraft foil (NASA CP 2046, V.II)
RAE 100	RAE100.DAT	
RAE 101	RAE101.DAT	
RAE 102	RAE102.DAT	
RAE 103	RAE103.DAT	
RAE 104	RAE104.DAT	
<i>VariEze Airfoils</i>		
VariEze wing bl23	VEZBL32.DAT	
VariEze winglet root	VEZWLTR.DAT	
VariEze winglet tip	VEZWLTT.DAT	
VariEze canard	VEZCAN.DAT	
<i>Human powered aircraft airfoils</i>		
DAE 11	DAE11.DAT	Daedalus airfoils (Mark Drela)
DAE 21	DAE21.DAT	
DAE 31	DAE31.DAT	
DAE 51	DAE51.DAT	(propeller foil?)
Lissaman 7769	LISS769.DAT	Gossamer Condor airfoil

Many other airfoils are available on the world wide web. In particular, the Applied Aerodynamics group at the University of Illinois, under the direction of Prof. Michael Selig, has established a massive online source for airfoil definitions and includes data from wind tunnel tests on the airfoils. Their focus is directed toward airfoils designed for low speeds and low Reynolds numbers, see <http://www.ae.uiuc.edu/m-selig/ads.html>. Finally, Richard Eppler has published an entire book of his airfoils, *Airfoil design and data*, Springer-Verlag, 1990.

The NASA low and medium speed airfoil program:

NASA Low Speed, Medium Speed, and natural Laminar Flow Airfoil Chart							
Airfoil Designation	Design Lift	Design Thickness	Design Mach	Test?	Ordinates in Airfoil Library?	Ref.	Comment
GA(W)-1	0.4/1.0	0.17		yes	yes	TN D-7428	Low Speed
LS(1)-0417mod		0.17			yes		"
GA(W)-2		0.13		yes	yes	TM X-72697	"
mod		0.13		yes	yes	TM X-74018	"
?		0.21		yes		TM 78650	"
LS(1)-0013		0.13		yes	yes	TM-4003	"
MS(1)-0313		0.13		yes	yes	TP-1498	Medium Speed
MS(1)-0317	0.30	0.17	0.68	yes	yes	TP-1786	"
mod		0.17		yes		TP-1919	"
NLF(1)-0215F	0.20?	0.15			yes	Raymer's Book	Natural Laminar Flow
NLF(1)-0414F					yes		"
NLF(1)-0416					yes		"
NLF(1)-0414F drooped L.E.					yes		"
NLF(2)-0415	0.40?	0.15?	?	yes	yes	Raymer's Book	"
HSNLF(1)-0213	0.20?	0.13?	?		yes	TM-87602	"
HSNLF(1)-0213 mod					yes		

The NASA Phase 2 supercritical airfoils are listed in the following chart.

NASA Supercritical Airfoils – Phase 2, from NASA TP 2969, March 1990, by Charles D. Harris							
Airfoil Designation	Design Lift	Design Thickness	Design Mach	Test?	Ordinates in Airfoil Library?	Ref.	Comment
SC(2)-0402	0.40	0.02			yes		
SC(2)-0403	0.40	0.03			yes		
SC(2)-0503	0.50	0.03			yes		
SC(2)-0404	0.40	0.04			yes		
SC(2)-0406	0.40	0.06			yes	unpubl.	
SC(2)-0606	0.60	0.06			yes		
SC(2)-0706	0.70	0.06	0.795	yes	yes	unpubl.	
SC(2)-1006	1.00	0.06		yes	yes	unpubl.	
SC(2)-0010	0.00	0.10			yes		
SC(2)-0410	0.40	0.10	0.785		yes		
SC(2)-0610	0.60	0.10	0.765		yes		
SC(2)-0710	0.70	0.10	0.755	yes	yes	TM X-72711	Airfoil 33
SC(2)-1010	1.00	0.10	0.70		yes		
SC(2)-0012	0.0	0.12		?	yes	TM-89102	
SC(2)-0412	0.40	0.12			yes		
SC(2)-0612	0.60	0.12			yes		
SC(2)-0712	0.70	0.12	0.735	?	yes	TM-86370	TM-86371
SC(2)-0414	0.40	0.14			yes		
SC(2)-0614	0.60	0.14			yes		
SC(2)-0714	0.70	0.14	0.715	Yes	yes	TM X-72712	Low Speed TM-81912
SC(2)-0518	1.00	0.18			yes		

Several transonic airfoils were developed at New York University by a group led by Paul Garabedian. The following table provides a list of the airfoils they published.

Garabedian and Korn Airfoil Chart							
Airfoil Designation	Design Lift	Design Thickness	Design Mach	Test?	Ordinates in Airfoil Library?	Pages in Ref., Korn II Book	Comment
79-03-12	0.293	0.123	0.790		yes	37,41-43	
72-06-16	0.609	0.160	0.720		yes	48,52-54	
71-08-14	0.799	0.144	0.710		yes	55,59-61	
70-10-13	0.998	0.127	0.700		yes	62,66-68	
65-14-08	1.409	0.083	0.650		yes	73,77-79	
65-15-10	1.472	0.104	0.650		yes	80,84-86	
82-06-09	0.590	0.092	0.820		yes	91,95	
75-06-12	0.629	0.117	0.750	yes	yes	96,99-101	the "Korn"
75-07-15	0.668	0.151	0.750		yes	102,106	

Their airfoils are included in:

Bauer, F., Garabedian, P., and Korn, D., *A Theory of Supercritical Wing Sections with Computer Programs and Examples*, Lecture Notes in Economics and Mathematical Systems, Vol. 66, Springer-Verlag, 1972.

Bauer, F., Garabedian, P., Jameson, A. and Korn, D., *Supercritical Wing Sections II, A Handbook*, Lecture Notes in Economics and Mathematical Systems, Vol. 108, Springer-Verlag, 1975.

Bauer, F., Garabedian, P., and Korn, D., *Supercritical Wing Sections III*, Lecture Notes in Economics and Mathematical Systems, Vol. 150, Springer-Verlag, 1977.

A.2 Classic Bodies of Revolution

Bodies of revolution form the basis for a number of shapes used in aerodynamic design and are also often used in comparing computational methods. The bodies defined in this section are generally associated with supersonic aerodynamics.

a. Summary of Relations

The body radius r is given as a function of x , $r/l = f(x/l)$. Once r is known, a number of other values characterizing the shape can be determined.

The cross-sectional area and derivatives are:

$$S(x) = \pi r^2 \quad (\text{A-39})$$

$$\frac{dS}{dx} = 2\pi r \frac{dr}{dx} \quad (\text{A-40})$$

$$\frac{d^2S}{dx^2} = 2\pi \left[\left(\frac{dr}{dx} \right)^2 + r \frac{d^2r}{dx^2} \right] \quad (\text{A-41})$$

Basic integrals are:

Volume,

$$V = \int_0^l S(x) dx \quad (\text{A-42})$$

Surface area,

$$S_{wet} = 2\pi \int_0^l r(x) dx \quad (\text{A-43})$$

Length along the contour,

$$p(\bar{x}) = \int_0^l \sqrt{1 + \left(\frac{dr}{dx} \right)^2} dx \quad (\text{A-44})$$

Note that the incremental values can be found by changing the lower limit of the integrals. The local longitudinal radius of curvature is given by:

$$R(x) = \frac{\left[1 + \left(\frac{dr}{dx} \right)^2 \right]^{3/2}}{\left| \frac{d^2r}{dx^2} \right|} \quad (\text{A-45})$$

Several simple shapes are also of interest in addition to those presented in detail. They are:

Parabolic Spindle:

$$\frac{r}{l} = 4 \frac{r_{mid}}{l} \frac{x}{l} \left(1 - \frac{x}{l} \right) \quad (\text{A-46})$$

Ellipsoid of revolution:

$$\frac{r}{l} = 2 \frac{r_{mid}}{l} \sqrt{\frac{x}{l} \left(1 - \frac{x}{l}\right)} \quad (\text{A-47})$$

and the power law body:

$$\frac{r}{l} = \frac{r_0}{l} \left(\frac{x}{x_N}\right)^n \quad (\text{A-48})$$

where x_N is the nose length, and r_0 is the radius at $x = x_N$. The nose is blunt for $0 < n < 1$.

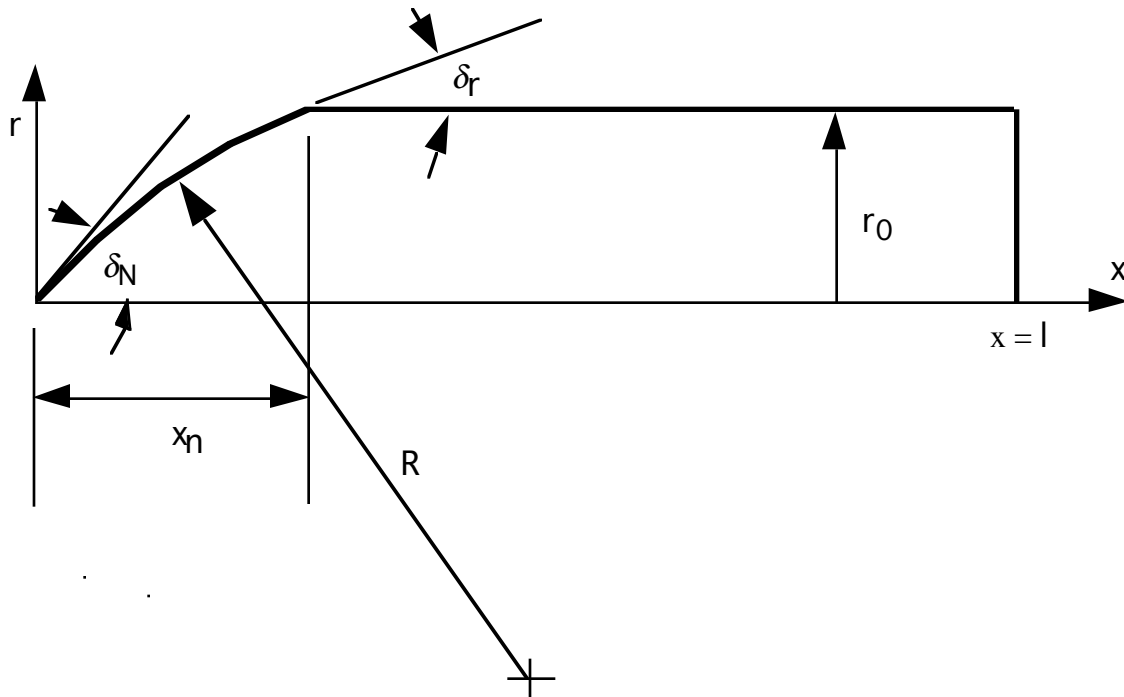
Another common shape is the spherical nose cap, and is discussed in detail in the reference by Krasnov. References that discuss geometry of bodies of revolution are:

Krasnov, N.F., *Aerodynamics of Bodies of Revolution*, edited and annotated by D.N. Morris, American Elsevier, New York, 1970.

Handbook of Supersonic Aerodynamics, Volume 3, Section 8, "Bodies of Revolution, NAVWEPS Report 1488, October 1961.

b). *Tangent/Secant Ogives*

The tangent or secant ogives are frequently used shapes in supersonic aerodynamics. The nomenclature is illustrated in the following sketch.



Note that the ogive is actually the arc of a circle and when $\delta_r = 0$ the ogive ends tangent to the body, so that $\delta_r = 0$ represents the tangent ogive body. If $\delta_r = \delta_N$, the cone-cylinder is recovered. If $\delta_r = 0$ and $\delta_N = 90^\circ$, the spherical cap case is obtained.

The expression for the radius r is determined using three basic constants for a particular case:

$$A = \frac{r_0}{l} \left(\frac{\cos \delta_N}{\cos \delta_r - \cos \delta_N} \right) \quad (\text{A-49})$$

$$B = 2 \frac{r_0}{l} \left(\frac{\sin \delta_N}{\cos \delta_r - \cos \delta_N} \right) \quad (\text{A-50})$$

and

$$C = \frac{r_0}{l} \quad (\text{A-51})$$

The radius is then given by:

$$\begin{aligned} \frac{r}{l} &= \sqrt{A^2 + B \left(\frac{x}{l} \right) - \left(\frac{x}{l} \right)^2} - A & 0 < \frac{x}{l} < \frac{x_N}{l} \\ &= C & \frac{x_N}{l} < \frac{x}{l} < 1 \end{aligned} \quad (\text{A-52})$$

where x_N is found as follows.

For a tangent ogive ($\delta_r = 0$), the ogive can be defined by specifying either x_N/r_0 or δ_N . The other value can then be found using:

Given δ_N ,

$$\frac{x_N}{r_0} = \frac{\sin \delta_N}{1 - \cos \delta_N} \quad (\text{A-53})$$

Or given x_N/r_0 ,

$$\delta_N = \cos^{-1} \left[\frac{\left(\frac{x_N}{r_0} \right)^2 - 1}{\left(\frac{x_N}{r_0} \right)^2 + 1} \right] \quad (\text{A-54})$$

For the secant ogive, the simplest analytical procedure is to define the ogive in terms of δ_N and δ_r , and then find x_N/l from:

$$\frac{x_N}{l} = \frac{r_0}{l} \left(\frac{\sin \delta_N - \sin \delta_r}{\cos \delta_r - \cos \delta_N} \right) \quad (\text{A-55})$$

If x_N/l is not satisfactory, δ_N and δ_r can be adjusted by trial and error to obtain the desired nose length. A program can be set up to handle this process quite simply.

The first and second derivatives are then given by:

$$\frac{d(r/l)}{d(x/l)} = \frac{B - 2(x/l)}{2[(r/l) + A]} \quad (\text{A-56})$$

and

$$\frac{d^2(r/l)}{d(x/l)^2} = -\frac{[B - 2(x/l)]^2}{4[(r/l) + A]^3} - \frac{1}{[(r/l) + A]} \quad (\text{A-57})$$

The relationships between radius and area derivatives given in section a) are then used to complete the calculation.

c) *The von Kármán Ogive*

The shape that produces minimum wave drag for a specified base area and length, according to slender body theory. This ogive has a very slightly blunted nose, and is described by Ashley and Landahl, *Aerodynamics of Wings and Bodies*, Addison-Wesley, 1965, pp. 178-181.

In this case it is convenient to work with the cross-sectional area and a new independent variable:

$$\theta = \cos^{-1} \left[2 \left(\frac{x}{x_N} \right) - 1 \right] \quad (\text{A-58})$$

or

$$\frac{x}{x_N} = \frac{1}{2}(1 + \cos \theta) \quad (\text{A-59})$$

where the nose is at $\theta = \pi$, and the base is located at $\theta = 0$.

Here we use x_N to denote the “nose length” or length of the ogive, and allow this shape to be part of an ogive-cylinder geometry.

The shape is then given as:

$$\frac{S(x)}{l^2} = \frac{S_B}{l^2} \left[1 - \frac{\theta}{\pi} + \frac{\sin 2\theta}{2\pi} \right] \quad (\text{A-60})$$

and

$$\frac{r}{l} = \sqrt{\frac{S/l^2}{\pi}} \quad (\text{A-61})$$

where S_B is the prescribed base area and l is the total length.

Defining

$$\bar{S} = \frac{S}{l^2}, \quad \bar{x} = \frac{x}{l}, \quad (\text{A-62})$$

We have

$$\frac{d\bar{S}}{d\theta} = -\frac{\bar{S}_B}{\pi} [1 - \cos 2\theta] \quad (\text{A-63})$$

$$\frac{d^2\bar{S}}{d\theta^2} = -\frac{2}{\pi} \bar{S}_B \sin 2\theta \quad (\text{A-64})$$

and

$$\frac{d\bar{S}}{d\bar{x}} = \bar{S}' = \frac{4}{\pi} \left(\frac{l}{x_N} \right) \bar{S}_B \sin \theta \quad (\text{A-65})$$

$$\frac{d^2\bar{S}}{d\bar{x}^2} = \bar{S}'' = -\frac{8}{\pi} \left(\frac{l}{x_N} \right)^2 \frac{\bar{S}_B}{\tan \theta}$$

The radius derivatives are then computed by:

$$\frac{d\bar{r}}{d\bar{x}} = \frac{\bar{S}'}{2\pi\bar{r}}, \quad \frac{d^2\bar{r}}{d\bar{x}^2} = \frac{\bar{S}''}{2\pi\bar{r}} - \frac{\bar{r}'^2}{\bar{r}} \quad (\text{A-66})$$

d) *The Sears-Haack Body*

This is the minimum wave drag shape for a given length and volume according to slender body theory. The body is closed at both ends and has a very slightly blunted nose, and is symmetric about the mid-point. It is described by Ashley and Landahl, *Aerodynamics of Wings and Bodies*, Addison-Wesley, 1965, pp. 178-181.

Although the notation used in section c) for the von Kármán Ogive section could be used, it is more common to describe the Sears-Haack body in the manner presented below. This form uses the fineness ratio, $f = l/d_{\max}$ to scale the shape. However, it is important to realize that the Sears-Haack shape is the minimum drag body for a specified volume and length, not for a specified fineness ratio. The minimum drag body for a specified fineness ratio is described below in section e) below.

Defining

$$\zeta = 1 - 2 \left(\frac{x}{l} \right), \quad (\text{A-67})$$

the Sears-Haack body is defined as

$$\frac{r}{l} = \frac{1}{2f} (1 - \zeta^2)^{3/4}. \quad (\text{A-68})$$

The derivatives are given by:

$$\frac{d(r/l)}{d(x/l)} = \frac{3\zeta}{1 - \zeta^2} \left(\frac{r}{l} \right) \quad (\text{A-69})$$

and

$$\frac{d^2(r/l)}{d(x/l)^2} = -\left(\frac{1}{1 - \zeta^2} \right) \left[\zeta \frac{d(r/l)}{d(x/l)} + 6 \left(\frac{r}{l} \right) \right]. \quad (\text{A-70})$$

The fineness ratio is related to the length and volume by:

$$f = \sqrt{\frac{3\pi^2 l^3}{64 V}}. \quad (\text{A-71})$$

In terms of f and either V or l , the other value can be found from the following:

Given f and l :

$$V = \frac{3\pi^2}{64} \frac{l^3}{f^2}. \quad (\text{A-72})$$

Given f and V :

$$l = \left[V \frac{64}{3\pi^2} f^2 \right]^{1/3}. \quad (\text{A-73})$$

The relationships between radius and area derivatives given in Section a) are then used to complete the calculation.

e) The Haack-Adams Bodies

The Haack-Adams bodies define a number of minimum drag shapes, as described by M.C. Adams in “Determination of Shapes of Boattail Bodies of Revolution for Minimum Wave Drag,” NACA TN 2550, November 1951. These bodies correspond to the following cases:

- I. Given length, base area, and contour passing through a specifically located radius.
- II. Given length, base area, and maximum area.
- III. Given length, base area, and volume.

In case I, the specified radius will not necessarily be the maximum radius.

The notation used in TN 2550 is employed in the equations, leading to the following definitions:

$$S = 4 \frac{\bar{S}(x)}{l^2}, \quad B = 4 \frac{S_{BASE}}{l^2}, \quad A = 4 \frac{S_A}{l^2}, \quad V = 8 \left(\frac{\bar{V}}{l^3} \right) \quad (\text{A-74})$$

where $S(x)$ is the area, S_A corresponds to either the specified area at a given location, or the maximum area, and V is the volume. The independent variable is defined with its origin at the body mid-point:

$$\zeta = 2 \left(\frac{x}{l} \right) - 1 \quad (\text{A-75})$$

and the location of the specified radius (Case I) and maximum radius (Case II) is designated C and given in ζ coordinates. When referred to the x coordinate, this value is designated C_x .

The equation for each case can be written in a standard form:

Case I — Given S_{BASE} , S_A , C_x :

$$\begin{aligned} \frac{\pi S}{B} = & \left[\frac{\pi A}{B} - \cos^{-1}(-c) \right] \frac{\sqrt{1-\zeta^2}(1-c\zeta)}{(1-c^2)^{3/2}} + \frac{\sqrt{1-\zeta^2}(\zeta-c)}{(1-c^2)} \\ & + \left[\frac{\pi A}{B} - \cos^{-1}(c) - c\sqrt{1-c^2} \right] \frac{(\zeta-c)^2}{(1-c)^2} \ln N + \cos^{-1}(-\zeta) \end{aligned} \quad (\text{A-76})$$

where

$$N = \frac{1 - c\zeta - \sqrt{1 - c^2} \sqrt{1 - \zeta^2}}{|\zeta - c|}. \quad (\text{A-77})$$

Case II — Given S_{BASE} , S_{MAX} :

First find the location of the maximum thickness from the implicit relation

$$f(c) = 0 = \frac{\pi A}{B} c - \sqrt{1 - c^2} - c \cos^{-1}(-c). \quad (\text{A-78})$$

Use Newton's iteration

$$c^{i+1} = c^i - \frac{f(c^i)}{f'(c^i)} \quad (\text{A-79})$$

where

$$f'(c) = \frac{\pi A}{B} - \cos^{-1}(-c). \quad (\text{A-80})$$

An initial guess of $c = 0$ is sufficient to start the iteration. Given c , the relation for the area is:

$$\frac{\pi S}{B} = \frac{\sqrt{1 - \zeta^2}}{c} + \frac{(\zeta - c)^2}{c\sqrt{1 - c^2}} \ln N + \cos^{-1}(-\zeta) \quad (\text{A-81})$$

where N is the same function as given in Case I.

Case III — Given S_{BASE} and V :

$$\frac{\pi S}{B} = \frac{8}{3} \left[\frac{V}{B} - 1 \right] \left((1 - \zeta^2)^{3/2} + \zeta \sqrt{1 - \zeta^2} + \cos^{-1}(-\zeta) \right) \quad (\text{A-82})$$

The maximum thickness for this case is located at:

$$e = \frac{1}{4(V/B - 1)} \quad (\text{A-83})$$

and in x coordinates

$$e_x = \frac{1}{2}(1 + e) \quad (\text{A-84})$$

Note that if $S_{BASE} = 0$, the Sears-Haack body is recovered.

A.3 Cross-Section Geometries for Bodies

The axisymmetric bodies described above can be used to define longitudinal lines for aerodynamic bodies. However, many aerodynamic bodies are not axisymmetric (the fuselage cross section is not round). In this section we define a class of cross section shapes that can be used to develop more realistic aerodynamic models. In particular, they have been used to study geometric shaping effects on forebody aerodynamic characteristics using an analytical forebody model with the ability to produce a wide variation of shapes. This generic model makes use of the equation of a super-ellipse to define cross sectional geometry. The super-ellipse, used previously to control flow expansion around wing leading edges, can recover a circular cross section, produce elliptical cross sections and can also produce chine-shaped cross sections. Thus it can be used to define a variety of different cross sectional shapes.

The super-ellipse equation for a cross section is:

$$\left(\frac{z}{b}\right)^{2+n} + \left(\frac{y}{a}\right)^{2+m} = 1 \quad (\text{A-85})$$

where n and m are adjustable coefficients that control the surface slopes at the top and bottom plane of symmetry and chine leading edge. The constants a and b correspond to the maximum half-breadth (the maximum width of the body) and the upper or lower centerlines respectively. Depending on the value of n and m , the equation can be made to produce all the shapes described above. The case $n = m = 0$ corresponds to the standard ellipse. The body is circular when $a = b$.

When $n = -1$ the sidewall is linear at the maximum half breadth line, forming a distinct crease line. When $n < -1$ the body cross section takes on a cusped or chine-like shape. As n increases, the cross-section starts to become rectangular.

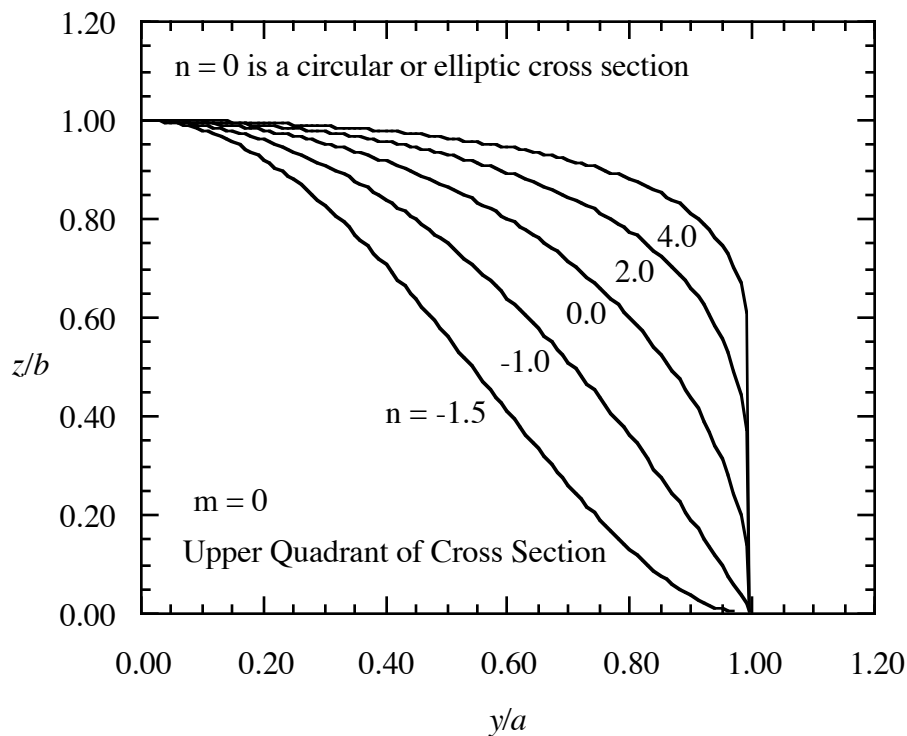
The derivative of z/b with respect to y/a is:

$$\frac{d\bar{z}}{d\bar{y}} = -\frac{\left(\frac{2+m}{2+n}\right)}{\left[1-\bar{y}^{(2+m)}\right]^{\frac{(1+n)}{(2+n)}}} \quad (\text{A-86})$$

where $\bar{z} = z/b$ and $\bar{y} = y/a$. As $\bar{y} \rightarrow 1$, the slope becomes:

$$\frac{d\bar{z}}{d\bar{y}} = \begin{cases} \infty & n > -1 \\ 0 & n < -1 \\ -(2+m)\bar{y}^{1+m} & n = -1 \end{cases} \quad (\text{A-87})$$

The following sketch shows a quadrant of the cross section for various values of n ranging from a chine to a rectangle.



Different cross sections can be used above and below the maximum half-breadth line. Even more generality can be provided by allowing n and m to be functions of the axial distance x . The parameters a and b can also be functions of the planform shape and varied to study planform effects. Notice that when $n = -1$ the value of m can be used to control the slope of the sidewall at the crease line. Also, observe that large positive values of n drive the cross section shape to approach a rectangular or square shape.

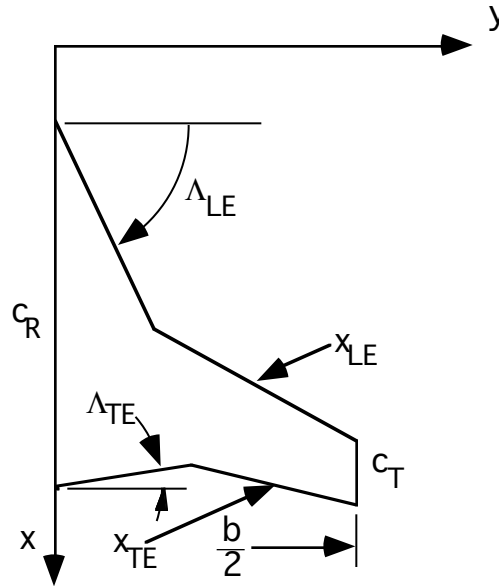
Connecting various cross section shapes is part of the subject of lofting, described in Chapter 9 of the Applied Computational Aerodynamics notes. One of the few other textbook discussions is contained in Raymer, *Aircraft Design: A Conceptual Approach*, published by the AIAA, in his Chapter 7. Dan Raymer worked at North American Aviation (actually Rockwell), where Liming* literally wrote the book on the analytic definition of aircraft lines.

* Roy Liming, *Practical Analytic Geometry with Applications to Aircraft*, MacMillan, New York, 1944. The book emphasizes conic sections, and the examples in the book are for the P-51 Mustang.

A.4 Planform Analysis

Several local and integral planform properties are of interest in aerodynamic analysis. They are summarized in this section. (Note: Biplanes use the total area of both wings as the reference area). For a more complete presentation see DATCOM.

The local values are the leading and trailing edge locations, $x_{LE}(y)$ and $x_{TE}(y)$, the local chord, $c(y)$, and the leading and trailing edge sweep angles: $\Lambda_{LE}(y)$ and $\Lambda_{TE}(y)$. The following sketch illustrates the standard nomenclature.



The integral properties are (assuming the planform is symmetric):

1. Planform Area, S

$$S = 2 \int_0^{b/2} c(y) dy \quad (\text{A-88})$$

2. Mean aerodynamic chord, \bar{c}

$$\bar{c} = \frac{2}{S} \int_0^{b/2} c^2(y) dy \quad (\text{A-89})$$

3. X position of centroid of area, x_{cen}

$$x_{cen} = \frac{2}{S} \int_0^{b/2} c(y) \left\{ x_{LE}(y) + \frac{c(y)}{2} \right\} dy \quad (\text{A-90})$$

4. Spanwise position of \bar{c}

$$y_{mac} = \frac{2}{S} \int_0^{b/2} y c(y) dy \quad (\text{A-91})$$

5. Leading edge location of *mac*.

$$x_{LE_{mac}} = \frac{2}{S} \int_0^{b/2} x_{LE}(y) c(y) dy \quad (A-92)$$

In addition, the following derived quantities are often of interest:

Aspect Ratio:

$$AR = \frac{b^2}{S_{ref}} \quad (A-93)$$

Average Chord:

$$c_A = \frac{S_{ref}}{b} \quad (A-94)$$

Taper Ratio:

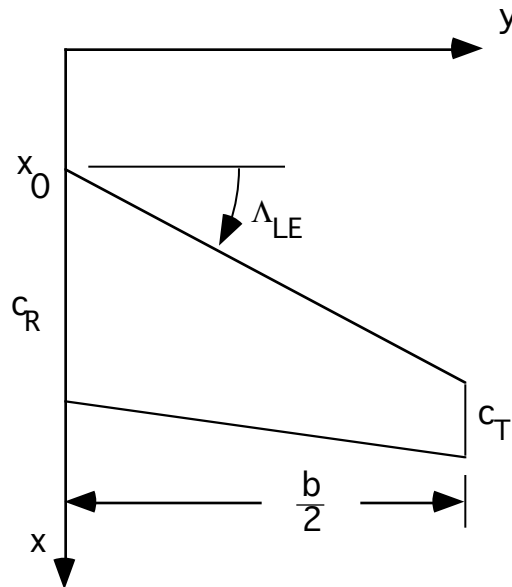
$$\lambda = \frac{c_T}{c_R} \quad (A-95)$$

S_{ref} is usually chosen to be equal to the area of a basic reference trapezoidal planform, and thus the actual planform area, S , may not equal S_{ref} .

When considering two areas, recall that the centroid of the combined surfaces is:

$$\begin{aligned} S\bar{x} &= S_1\bar{x}_1 + S_2\bar{x}_2 \\ S\bar{y} &= S_1\bar{y}_1 + S_2\bar{y}_2 \end{aligned} \quad (A-96)$$

For a standard trapezoidal wing it is convenient to collect the following formulas, where the sketch shows the nomenclature:



$$\begin{aligned} x_{LE}(y) &= x_{LE_0} + y \tan \Lambda_{LE}(y) \\ x_{TE}(y) &= x_{TE_0} + y \tan \Lambda_{TE}(y) \end{aligned} \quad (A-97)$$

and the local chord is:

$$\frac{c(y)}{c_R} = 1 - (1 - \lambda)\eta \quad (\text{A-98})$$

where:

$$y = \frac{b}{2}\eta \quad \text{or} \quad \eta = \frac{y}{b/2} \quad \text{and} \quad \lambda = \frac{c_T}{c_R}. \quad (\text{A-99})$$

The sweep at any element line can be found in terms of the sweep at any other by:

$$\tan \Lambda_n = \tan \Lambda_m - \frac{4}{AR} \left[(n - m) \left(\frac{1 - \lambda}{1 + \lambda} \right) \right] \quad (\text{A-100})$$

where n, m are fractions of the local chord. An alternate formula is available using the trailing edge sweep angle:

$$\tan \Lambda_n = (1 - n) \tan \Lambda_{LE} + n \tan \Lambda_{TE} \quad (\text{A-101})$$

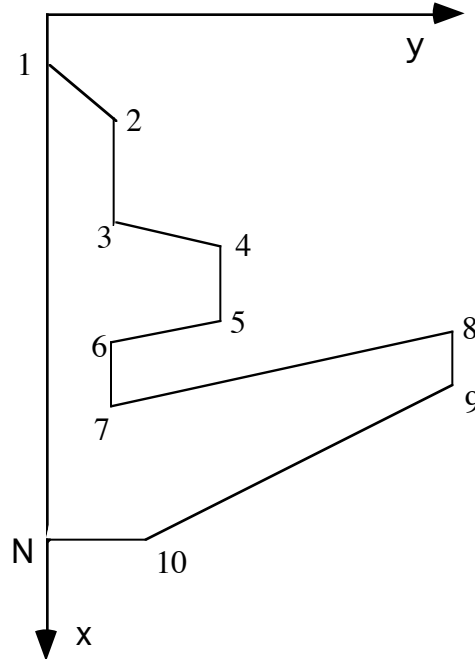
The integral and other relations are given by:

$$\begin{aligned} S &= \frac{b}{2} c_R (1 + \lambda) \\ c_{ave} &= \frac{S}{b} \\ \frac{\bar{c}}{c_R} &= \frac{2}{3} \left(\frac{1 + \lambda + \lambda^2}{1 + \lambda} \right) \\ AR &= \frac{b^2}{S} = \frac{b/2}{c_R} \left(\frac{4}{1 + \lambda} \right) \\ y_{mac} &= \frac{b}{6} \left(\frac{1 + 2\lambda}{1 + \lambda} \right) \\ \frac{x_{LE_{mac}}}{c_R} &= \frac{x_{LE_0}}{c_R} + \left(\frac{1 + 2\lambda}{12} \right) AR \tan \Lambda_{LE} \\ x_{cen} &= x_{LE_{mac}} + \frac{\bar{c}}{2} \end{aligned} \quad (\text{A-102})$$

When computing the projected planform area of an entire configuration, the following formula is useful:

$$S = \sum_{k=1}^{k=N} (y_{k+1} + y_k)(x_{k+1} - x_k) \quad (\text{A-103})$$

where the sketch below defines the nomenclature.



At $k = N$, y_{k+1}, x_{k+1} refer to the initial points y_1, x_1 . For normal planforms, $y_{n+1} = y_1 = 0$, so that the summation can be terminated at $N-1$. This formula assumes planform symmetry and provides the total planform area with only one side of the planform used in the computation.

A.4.1 A note on reference chords and aerodynamic center location

Looking at the aerodynamics literature, especially the older literature and textbooks, you find that the nomenclature for reference chords is not uniform. However, there is a standard in use today in the US industry. The issue is what value to use when nondimensionalizing the pitching moment:

$$C_m = \frac{M}{qS_{ref}c_{ref}} \quad (A-104)$$

The USAF DATCOM defines the standard. They define c_{ref} to be the *mean aerodynamic chord* or *mac*:

$$\bar{c} = \frac{2}{S} \int_0^{b/2} c^2(y) dy \quad (A-89)$$

Which for a straight tapered wing is:

$$\frac{\bar{c}}{c_r} = \frac{2}{3} \left(\frac{1 + \lambda + \lambda^2}{1 + \lambda} \right) \quad (A-102)$$

The use of the symbol \bar{c} to represent the *mean aerodynamic chord* is confusing because \bar{c} is sometimes used to represent the average chord, $c_a = S/b$ in other literature. For example, ESDU

Item 76003 uses \bar{c} to be the standard (or geometric) mean chord, that I have defined here as the average chord. They use $\bar{\bar{c}}$ as the *mac* defined by Eqn. A-89. The main problem occurs when the report or paper does not specifically define the terms used. For example, Lamar and Alford (1966) use Eqn. A-89 to nondimensionalize the pitching moment, but they call it the mean geometric chord.

Another issue to be aware of is that the *mac* does not necessarily lie on the actual planform if the wing is not a simple straight tapered configuration.

A.5 Conical Camber

An important class of camber distributions is associated with the planform, and not the airfoil. Conical camber has been widely used. Many forms have been used, however the NACA defined a specific type of conical camber that is known as NACA conical camber. The most recent example of NACA conical camber is the F-15 wing. It improves the drag characteristics of wings in the subsonic and transonic flow region even though it was developed to reduce the drag at supersonic speeds!

The key references are:

Hall, C.F., "Lift, Drag, and Pitching Moment of Low Aspect Ratio Wings at Subsonic and Supersonic Speeds," NACA RM A53A30, 1953.

This report provided the original mathematical definition of NACA conical camber. It also provided a large range of test conditions for which the camber was effective.

Boyd, J.W., Migotsky, E., and Wetzel, B.E., "A Study of Conical Camber for Triangular and Swept Back Wings," NASA RM A55G19, Nov. 1955.

This report provided more details of the derivation of the formulas for NACA conical camber, and corrected errors in the equations presented in the first report. Additional experimental results were also presented.

An advanced form of conical camber addressing so-called supercritical crossflows cases is Supercritical Conical Camber (SC3). It is described in: Mason, W.H., "A Wing Concept for Supersonic Maneuvering," NASA CR 3763, Dec. 1983 (see also AIAA Paper 83-1858, July, 1983).

A.6 Three-Dimensional Wing Geometry

Wing geometry is often defined by interpolating between airfoil section-specified at particular spanwise stations. Some care some be taken to interpolate properly. See Chapter 9, Geometry and Grids, in the Applied Computational Aerodynamics notes for a discussion of wing lofting. Program WNGFLT is described in App. E, Utility Codes. This program provides an example of a lofting scheme to provide wing ordinates at any desired location. It can be used to provide wing ordinates for a wide class of wings. It in fact will produce a very good approximation to the wing design employed by a successful Navy airplane.